# Impact of aircraft emissions on $NO_x$ in the lowermost stratosphere at northern midlatitudes

Y. Kondo[1], M. Koike[1], H. Ikeda[1], B.E. Anderson[2], K.E. Brunke[3], Y. Zhao[1], Kita[4], T. Sugita[5], H.B Singh[6], S.C. Liu[7], Jeagle[8], A. Thompson[9], G.L. Gregory[2], R. Shetter[10], G. Sachse[2], E.V. Browell[2], M.J. Mahoney[11].

[1] Nagoya University, Toyokawa, Japan.

[2] NASA Langley Research Center, Hampton, VA

[3] Chistopher Newport University, Newport News, VA

[4] University of Tokyo, Tokyo, Japan

[5] National Institute for Environmental Studies, Tsukuba, Japan.

[6] NASA Ames Research Center, Moffett Field, CA

[7] Georgia Institute of Technology, Atlanta, GA

[8] Harvard University, Cambridge, MA

[9] NASA Goddard Space Flight Center, MD

[10] National Center for Atmospheric Research

[11] Jet Propulsion Laboratory, Pasadena, CA

Short title: AIRCRAFT IMPACT ON $NO_x$

To be submitted to the Geophysical Research Letters, January 4, 1999

***Abstract.*** Airborne measurements of NO, total reactive nitrogen ($NO_y$), $O_3$, and condensation nuclei (CN) were made, together with other tracers such as CO and $H_2O$, within air traffic corridors over the U.S. and North Atlantic regions in October and November 1997. $NO_x$ (= NO + $NO_2$) and $NO_y$ data obtained in the lower stratosphere were examined using the calculated increase in $NO_y$ ($\Delta NO_y$) along five-day trajectories as a parameter to identify possible effects of aircraft on reactive nitrogen. The mixing ratio of CN, which is emitted from aircraft, was also used as an independent parameter to analyze the impact of aircraft on $NO_x$. The values of $NO_x$ and $NO_x/NO_y$ ratio were positively correlated with these parameters. In addition, the relationship between $NO_x$ and CN was close to that observed in aircraft plumes encountered during SONEX and other aircraft observations. These results indicate that the $NO_x$ values were enhanced by aircraft emissions. The background values of $NO_x$ and $NO_x/NO_y$ ratio were determined as the values for $\Delta NO_y = 0$. Based on these background values, aircraft emissions were estimated to have increased the $NO_x$ levels by 80 % on average in the corridor region over the US and north Atlantic.

## Introduction

Active nitrogen ($NO_x = NO + NO_2$) plays a crucial role in the photochemistry of ozone in the upper troposphere (UT) and lowermost stratosphere (LS). In these regions, $NO_x$ acts as a catalyst to produce ozone photochemically [*Singh et al.*, this issue].

Major sources of $NO_x$ in the UT are convective transport of $NO_x$ from the lower troposphere, production by lightning, emissions from aircraft, and transport from the stratosphere. Aircraft emissions may be more important in determining $NO_x$ levels in the LS than in the UT since the transport of tropospheric $NO_x$ into the stratosphere is quite limited. However, the impact of aircraft on large-scale distribution of $NO_x$ in the LS is still poorly known. Meridional distributions of $NO_x$ and $NO_y$ ranging between 40-90 °N were measured in the LS mostly in winter on board the DC-8 during the Airborne Arctic Stratospheric Expedition (AASE) I [*Carroll et al.*, 1990] and II [*Weinheimer et al.*, 1994; *Witte et al.*, 1997]. Decreases in the $NO_x$ mixing ratios from 40 °N to the polar region were observed. Aircraft measurements of $NO_x$ and other tracers were made over the eastern North Atlantic in the air traffic corridor region in November [*Schlager et al.*, 1997]. Most of the $NO_x$ peaks attributed to air traffic were observed in the UT and only a small portion of the measurements was made in the LS. During the SASS Ozone and $NO_x$ Experiment (SONEX), reactive nitrogen and a number of tracers were measured over the US continent and North Atlantic Ocean, where $NO_x$ emissions from commercial aircraft are believed to be the greatest [*Singh et al.*, this issue]. The purpose of this study was to understand the effect of aircraft on $NO_x$ in the LS over these regions.

## Aircraft Observations

The SONEX mission was carried out using the NASA Ames Research Center's Douglas DC-8 aircraft from October 7 to November 12, 1997. A total of 16 flights were completed over the US continent and Atlantic Ocean. A list of the equipment used for the SONEX measurements and the locations of the flights are found in *Singh et al.* [this issue]. The mixing ratios of NO, $NO_x$, $NO_y$, $O_3$, CO, $H_2O$, and CN were the key parameters used for the present analysis. Assuming the photostationary state the $NO_2$ values were calculated using the mixing ratios of NO and $O_3$, and the $NO_2$ photolysis rates observed at solar zenith angles lower than 87°. The uncertainties in the $NO_2$ and $NO_x$ values above 7 km were about ±30 and ±10 %, respectively. Concentrations of volatile (fine CN) and nonvolatile CN with diameters larger than 18 nm were measured with a precision of ±10 % using the two separate CN counters as described in *Anderson et al.* [1998a, 1998b]. The observed concentrations in number of particles $cm^{-3}$ at an ambient pressure and temperature were normalized to number per standard $cm^3$ (0 °C and 1013 hPa) to represent the CN mixing ratio.

## Results and Discussion

The aircraft measurements in the NAFC region showed simultaneous enhancements in the $NO_y$ and CN levels lasting from a few seconds to 100 seconds. On 252 occasions, $NO_y$ enhancements exceeding 100 pptv above the background levels were identified as due to aircraft emissions in the UT and the LS [*Anderson et al.*, this issue]. The median durational value of the $NO_y$ and CN levels was 13 seconds, corresponding to an aircraft plume with a width of 3 km. These spike data were excluded from the analysis described below, although the screening of the data did not alter the statistical results. A dynamical simulation has shown that aircraft plumes disperse to 4 km in width about one hour following the emissions [*Dürbeck and Gerz*, 1996]. This means that plumes having existed less than several hours were excluded from the present analysis.

In the present analysis, we used all the LS data obtained during SONEX with $O_3$ mixing ratios higher than 100 ppbv. The $O_3$ values higher than 200 ppbv were observed most frequently north of 65 °N because of a mean tropopause height as low as 8.5 km. Associated with the tropopause folding, air masses with $O_3$ values higher than 100 ppbv were transported well below the tropopause height, which was determined from the temperature and $O_3$ profiles obtained by the Microwave Temperature Profiler (MTP) and UV lidar (DIAL). This data was also excluded.

The $NO_x$ mixing ratios increased by a factor of 3.5 on average for the $O_3$ values between 25 and 125 ppbv. The increase in the $NO_x$ mixing ratios in this $O_3$ range was associated with a corresponding increase in the $NO_y$ values, resulting in nearly constant $NO_x/NO_y$ ratios of 0.25. By contrast, the median $NO_y$ values increased by only 15 % and 50 % for the $O_3$ ranges of $100 < O_3 < 200$ ppbv and $100 < O_3 < 350$ ppbv, respectively. Accordingly, the changes in the $NO_x$ mixing ratios were reflected directly in the $NO_x/NO_y$ ratios in the LS. The median $NO_x$ levels showed a sharp decrease at an $O_3$ mixing ratio of 200 ppbv. Given the $NO_x$ dependence on $O_3$, the analysis below was made for the two ranges, $100 < O_3 < 200$ ppbv and $200 < O_3 < 350$ ppbv. The decrease

in the $NO_x/NO_y$ ratio with increases in the $NO_y$ and $O_3$ values was also observed in the Arctic UT and LS during AASE I [*Carroll et al.*, 1990]. Where $O_3 > 100$ ppbv, the CO mixing ratios were lower than 90 ppbv, indicating that the LS air was not significantly influenced by highly polluted tropospheric air.

Figure 1a shows the profiles of the 10-second averaged values of $NO_x$ obtained in the LS during the entire SONEX measuring period, together with the median values for each 1 km step. In this figure two profiles for the different $O_3$ ranges are given. Between 8.5 and 11.5 km, the $NO_x$ mixing ratios often showed enhanced values. The median $NO_x$ values above 10 km were higher than those below 8 km by a factor of 3-4 where $100 < O_3 < 200$ ppbv. Similar to the $NO_x$ mixing ratios, the CN mixing ratios above 10 km (not shown) were larger than those below 8 km by a factor of 2-2.5. Inasmuch as commercial air traffic was the busiest between 8.7 km and 12.3 km, the increases in the $NO_x$ and CN mixing ratios at these altitudes suggest the influence of aircraft on these species. In accord with the present CN data, thin layers of highly concentrated CN were often observed in the same altitude region by balloon-borne CN counters launched from Laramie, Wyoming (41 °N, 106 °W) [*Hofmann et al.*, 1998]. By contrast, where $O_3 > 200$ ppbv, the median values of $NO_x$ and CN did not show any enhancement between 8.5 and 11.5 km.

In order to understand the impact of air traffic on the variability of the $NO_x$ levels more quantitatively, increases in the $NO_x$ mixing ratios along five-day kinematic trajectories were calculated by integrating the $NO_x$ molecules emitted from aircraft into these air masses. For this calculation, the monthly mean $NO_x$ emission distribution from the ANCAT/EC2 emission inventory [*Gardner*, 1998] was used. The ANCAT/EC2 emission inventory, which is very similar to the NASA inventory [*Baughcum et al.*, 1996], is given at each one degree grid point in latitude and longitude with a vertical resolution of 1 km. The trajectories were calculated using the European Centre for Medium-Range Weather Forecasts (ECMWF) gridded data. During transport, part of the

$NO_x$ emitted from aircraft is oxidized to reservoir species such as $HNO_3$ and $HNO_4$ by the reactions with OH and $HO_2$. Hydrolysis of $N_2O_5$ on sulfate aerosols also converts $NO_x$ into $HNO_3$. The total increase in the calculated $NO_x$ abundance assuming no chemical loss represents the increase in $NO_y$ and therefore is denoted as $\Delta NO_y$.

The $\Delta NO_y$ profiles are shown in Figure 1b. Where $100 < O_3 < 200$ ppbv, the $\Delta NO_y$ values above 10 km were significantly higher than those below, consistent with the $NO_x$ and CN profiles. The peak median $\Delta NO_y$ value at 10-12 km was about 100 pptv, which represents a significant portion of the $NO_x$ value observed at the same altitudes. The $\Delta NO_y$ values where $O_3 > 200$ ppbv were lower than those where $100 < O_3 < 200$ ppbv by a factor of 2-4, due to light air traffic north of 65 °N. Therefore the $O_3$ dependence of the $\Delta NO_y$ values partly explains the dependence of the $NO_x$ and CN values on the $O_3$ values.

The observed values of $NO_x$ are directly compared with $\Delta NO_y$ in Figure 2. For this comparison data obtained above 9.5 km was used. Similar comparisons were also made for the values of the $NO_x/NO_y$ ratio and CN. The $NO_x$ and CN mixing ratios and the $NO_x/NO_y$ ratios increased with $\Delta NO_y$, expressed by the following equations:

$$[NO_x] = 89 + 0.849\ [\Delta NO_y] \qquad (r^2 = 0.51) \qquad (1)$$

$$NO_x/NO_y = 0.131 + 0.000988\ [\Delta NO_y] \qquad (r^2 = 0.53) \qquad (2)$$

$$[CN] = 833 + 6.15\ [\Delta NO_y] \qquad (r^2 = 0.37) \qquad (3)$$

Here $[NO_x]$ and $[\Delta NO_y]$ are expressed in units of pptv and [CN] is expressed in the unit of number STP $cm^{-3}$. The square of the correlation coefficient is given as $r^2$. The majority of the LS data was obtained at 10-12 km and the equations (1)–(3) represent this

altitude range. The number of days the air mass took to reach 50 % of the $\Delta NO_y$ values is also shown in Figure 2. It can be seen that injection of $NO_y$ occurred rather uniformly over the five-day period. For the $\Delta NO_y$ values of 100–150 pptv with the most recent aircraft injections, the effect of chemical conversion of $NO_x$ should be at a minimum. Even for this data, the scatter of the observed $NO_x$ values ranged from 100 to 300 pptv, partly due to an error in estimating the $\Delta NO_y$ values from the ANCAT/EC2 data.

The slope in equation (1) is close to 1, suggesting that a significant portion of $\Delta NO_y$ remained in the form of $NO_x$. The $NO_x/NO_y$ ratio dependence on $\Delta NO_y$ is also significant with an $r^2$ value very similar to that for $NO_x$, a result consistent with the median $NO_y$ values changing by only 15 % in the $100 < O_3 < 200$ range, as discussed above.

The $NO_x$ values where $O_3 > 200$ ppbv are expressed as a function of $[\Delta NO_y]$ by the following equation:

$$[NO_x] = 31 + 0.805\ [\Delta NO_y] \qquad (r^2 = 0.45) \qquad (4)$$

The $NO_x$ values expressed by this equation are about 60 pptv lower than those by equation (1) on average, although the slopes of both equations are similar. Similarly, the $NO_x/NO_y$ ratios where $O_3 > 200$ ppbv were also lower than those where $100 < O_3 < 200$ ppbv by about 0.1. The $O_3$ values higher than 200 ppbv were often observed north of 65 °N as discussed above. At higher latitudes, decreased solar radiation combined with more rapid formation of $N_2O_5$ due to higher $O_3$ mixing ratios can enhance the $NO_x$ oxidation rate, leading to lower $NO_x$ values.

In addition to $\Delta NO_y$, the CN mixing ratio may also serve as a parameter by which to characterize the degree of the effect of aircraft on $NO_x$. It is free from the uncertainty of

the emission inventory associated with the $\Delta NO_y$ estimate since $NO_x$ and CN are emitted from aircraft simultaneously. First, the relationship between enhanced levels of $NO_y$ ($\delta NO_y$) and CN ($\delta CN$) in aircraft plumes was derived. The $\delta NO_y/\delta CN$ ratios were scattered between 0.04 and 0.2 and the median value was 0.097 pptv $cm^{-3}$. The wide range in the $\delta NO_y/\delta CN$ ratios reflects the variability in the emission indices (EI's) of CN and $NO_2$, depending on various parameters, including the type of the engine, sulfur content in the fuel, and fuel flow [*Miake-Lye, et al.*, 1998; *Hagen et al.*, 1998; *Anderson et al*, 1998a and 1998b]. Assuming an $NO_2$ EI of 11 g/kg (fuel burned), the $\delta NO_y/\delta CN$ ratio of 0.097 pptv $cm^{-3}$ corresponds to a CN EI of $5.5 \times 10^{16}$ particles/kg (fuel burned). This value falls within the range of the values obtained by the aircraft measurements during SUbsonic aircraft: Contrails and Cloud Effects Special Study (SUCCESS) [*Anderson et al*, 1998a and 1998b].

The 10 s averaged values of $NO_x$ obtained above 9.5 km where $100 < O_3 < 200$ ppbv are plotted versus the CN mixing ratios in Figure 3. For comparison, the median relationship of $\delta NO_y/\delta CN = 0.097$ pptv $cm^{-3}$ is also shown. The $NO_x$ values were positively correlated with the CN mixing ratio. In addition, the average relationship between $NO_x$ and CN was very close to that observed in aircraft plumes.

During SUCCESS, aircraft engines were observed to emit volatile particles much more abundantly than nonvolatile particles [*Anderson et al.*, 1998a, 1998b, 1999; *Paladino et al.*, 1998]. The $NO_x$ mixing ratios are plotted versus the ratios of concentrations of nonvolatile to total fine CN (nonvolatile/total fine CN) in Figure 4. For comparison, the median $\delta NO_y$ values in the aircraft plumes are plotted versus the nonvolatile/total CN ratios of $0.05 \pm 0.05$ and $0.15 \pm 0.05$, respectively. The $NO_x$ values are anti-correlated with the nonvolatile/total CN ratio. The nonvolatile/total CN

ratio was 0.2 where $NO_x$ = 200 pptv increasing to 0.4 ± 0.1 where $NO_x$ = 80 pptv. It is also seen that the nonvolatile/total CN ratios higher than 0.4 were dominated by air masses with $\Delta NO_x$ values lower than 100 pptv. In the aircraft plumes, the $\delta NO_y$ values also decreased with the increase of the nonvolatile/total fine CN ratios. These values are close to those extrapolated from the non-plume data.

The similarity in the $NO_x$–CN correlation in the LS air and aircraft plumes was caused by the order of magnitude similarity in the lifetimes of $NO_x$ and CN. After being emitted from aircraft at 10 km, $NO_x$ is oxidized to higher-oxide nitrogen, primarily to $HNO_3$ with a time constant of about 1-2 weeks in the $100 < O_3 < 200$ ppbv region. On the other hand, CN is lost primarily through coagulation with CN for CN mixing ratios higher than 500 $cm^{-3}$. The half-lifetime of CN with a diameter of 18 nm at a CN mixing ratio of 1000 $cm^{-3}$ is about two days and decreases inversely in the CN mixing ratio [*Pruppacher and Klett*, 1997]. The $NO_x$ and CN are transported from the LS to the troposphere in two weeks time [*Schoeberl et al.*, 1998], limiting the ultimate age of the aircraft-affected air.

$NO_x$ has sources in the troposphere other than emissions from aircraft as discussed in the introduction. Similarly, CN is also produced in the troposphere by processes including condensation of sulfuric acid. In addition to aircraft emissions, the mixing of tropospheric air high in $NO_x$ and CN into the stratosphere might have contributed to the positive $NO_x$–CN and $NO_x/NO_y$–CN correlations. However, it is unlikely that this process had a pronounced effect on the observed correlations given that the $NO_x$ mixing ratios failed to show significant correlation with either the CO or $H_2O$ mixing ratios (not shown). Similarly, CN failed to show significant correlation with either CO or $H_2O$. In turn, the CO and $H_2O$ mixing ratios observed during SONEX generally decreased with the $O_3$ mixing ratios as expected from the tropospheric-stratospheric exchange. Therefore, it is unlikely that the enhanced levels of $NO_x$ and CN in the LS were primarily

caused by transport of these species from the troposphere.

The increase in the $NO_x$ values due to aircraft exhaust over the US continent and in NAFC can be estimated using two independent parameters which characterize the impact of aircraft emissions: $\Delta NO_y$ and CN mixing ratios. From equations (1) – (3), the background values of CN, $NO_x$, and $NO_x/NO_y$ ratio where $100 < O_3 < 200$ ppbv are defined as $833 \pm 310$ $cm^{-3}$, $89 \pm 37$ pptv, and $0.13 \pm 0.052$, respectively, as the values for $\Delta NO_y = 0$. On the other hand, the median values of $NO_x$ and $NO_x/NO_y$ ratio where CN was between 500 and 1000 $cm^{-3}$ were $95 \pm 30$ pptv and $0.14 \pm 0.046$, respectively. These $NO_x$ and $NO_x/NO_y$ values are close to those determined from equations (1) and (2). The median and average values of CN, $NO_x$, and $NO_x/NO_y$ ratio are summarized in Table 1, together with the background values. Based on these values, we estimated the aircraft emissions to have increased the values of CN, $NO_x$, and $NO_x/NO_y$ ratio by 460 $cm^{-3}$, 79 pptv, and 0.10, respectively, on average. These values correspond to increases in CN and $NO_x$ by about 55 and 80 % above the background, respectively. A significant portion of the $NO_x$ values was in the range of 200–300 pptv, corresponding to an aircraft impact of a factor of 3.

## Conclusions

It is very likely that aircraft emissions had a significant impact on the $NO_x$ levels in the LS over the US continent and North Atlantic Ocean inasmuch as the $NO_x$ and mixing ratios above 9.5 km were significantly correlated with the independent parameters of aircraft emissions, i.e., $\Delta NO_y$ levels, CN values, and nonvolatile/total CN ratios. In order to estimate quantitatively the impact of aircraft emissions on $NO_x$ and CN, the background levels of CN, $NO_x$ and $NO_x/NO_y$ ratios where $100 < O_3 < 200$ ppbv were derived from the correlations of these quantities with $\Delta NO_y$. The aircraft emissions are estimated to have increased the values of $NO_x$ and $NO_x/NO_y$ ratio by 79 pptv and 0.10 on average, which corresponds a 80–90 % overall increase.

***Acknowledgments.*** This work was supported by the SASS Program at NASA. We wish to thank the flight and ground crew of the NASA Ames Research Center for their DC-8 aircraft operations. We would also like to thank N. Toriyama, T. Kurimoto, M. Kanada, H. Jindo, and P. Yue for their assistance in instrument construction, laboratory tests, preparation of experiments, and data processing. The lifetime of CN was calculated by B. Liley. This work was partially supported by the Japanese Ministry of Education, Science and Culture.

## References


Anderson, B.E., et al., *Geophys. Res. Lett.,* this issue.

Anderson, B.E., W.R. Cofer, J.D. Barrick, D.R. Bagwell, and C.H. Hudgins, Airborne observations of aircraft aerosol emissions I: Total nonvolatile particle emission indices, *Geophys. Res. Lett., 25*, 1689-1692, 1998a.

Anderson, B.E., W.R. Cofer, J.D. Barrick, D.R. Bagwell, and C.H. Hudgins, Airborne observations of aircraft aerosol emissions II: Factors controlling volatile particle production, *Geophys. Res. Lett., 25*, 1693-1696, 1998b.

Baughcum, S.L., T.G. Tritz, S.C. Henderson, and D.C. Pickett, Scheduled civil aircraft emission inventories for 1992: Database development and analysis, *NASA Contract Rep., CR-4700*, April, 1996.

Gardner, R.M. (Ed), ANCAT/EC2 aircraft emission inventories 1991/1992 and 2015: Final report, Produced by the ECAC/ANCAT and EC working group, 1998.

Carroll, M.A., D. Montzka, G. Hübler, K.K. Kelly, and G.L. Gregory, In situ measurements of $NO_x$ in the airborne Arctic stratospheric expedition, *Geophys. Res. Lett., 17*, 493-496, 1990.

Dürbeck, T., and T. Gerz, Dispersion of aircraft exhausts in the free atmosphere, J. *Geophys. Res., 101*, 26007-26-15, 1996.

Hagen, D., P. Whitefield, J. Paladino, M. Trueblood, and H. Lienfield, Particulate sizing and emission indices for a jet engine exhaust sampled at cruise, *Geophys. Res. Lett., 25*, 1681-1684, 1998.

Hofmann D.J., R.S. Stone, M.E. Wood, T. Deshler, J.M. Harris, An analysis of 25 years of balloonborne aerosol data in search of a signature of the subsonic commercial aircraft fleet, *Geophys. Res. Lett., 25*, 2433-2436, 1998.

Jaegle, L., *et al.*, Sources and chemistry of $NO_x$ in the upper troposphere over the United States, *Geophys. Res. Lett., 25*, 1705-1708, 1998.

Kotamarthi, V.R., *et al.*, Evidence of heterogeneous chemistry on sulfate aerosols in

stratospherically influenced air masses sampled during PEM-West B, *J. Geophys. Res., 102*, 28452-28436, 1997.

Miake-Lye, R.C., *et. al.*, SOx oxidation and volatile aerosol in aircraft exhaust plumes depend on fuel sulfur content, *Geophys. Res. Lett., 25*, 1677-1680, 1998.

Paladino, J., P. Whitefield, D. Hagen, A.R. Hopkins, and M. Trueblood, Particle concentration characterization for jet engine emissions under cruise conditions, *Geophys. Res. Lett., 25*, 1697-1700, 1998.

Pruppacher, H.R., and J.D. Klett, Microphysics of clouds and precipitation, Kluwer Academic Publications, 1997.

Singh, H.B., A.M. Thompson, and H. Schlager, 1997 SONEX Airborne Mission: Overview and accomplishments, *Geophys. Res. Lett.*, this issue.

Schlager, H., *et al.*, In situ observations of air traffic emission signatures in the North Atlantic flight corridor, *J. Geophys. Res., 102*, 10739-10750, 1997.

Schoeberl, M.R., C.H. Jackman, and J.E. Rosenfield, A Lagrangian estimate of aircraft effluent lifetime, *J. Geophys. Res., 103*, 10817-10825, 1998.

Weinheimer, A., *et al.*, Meridional distribution of $NO_x$, $NO_y$, and other species in the lower stratosphere and upper troposphere during AASE II, *Geophys. Res. Lett., 21*, 2583-2586, 1994.

Witte, J.C, I.A. Folkins, J. Neima, B.A. Ridley, J.G. Walega, and A.J. Weinheimer, Large-scale enhancements in $NO/NO_y$ from subsonic aircraft emissions: Comparisons with observations, *J. Geophys. Res., 102*, 28169-28175, 1997.

Author addresses

H. Ikeda, M. Koike, Y. Kondo, and Y. Zhao, Solar-Terrestrial Environment Laboratory, Nagoya University, 3-13 Honohara, Toyokawa 442-8507, Aichi, Japan. (e-mail: kondo@stelab.nagoya-u.ac.jp)

B.E. Anderson, E.V. Browell, G.L. Gregory, G.W. Sachse, Atmospheric Science

Division, NASA Langley Research Center, Hampton, VA 23681.

K.E. Brunke, Department of Biology, Chemistry, and Environment Science, Chistopher Newport University, Newport News, VA.

K. Kita, Department of Earth and Planetary Physics, Graduate School of Science, University of Tokyo, Tokyo 113, Japan.

T. Sugita, National Institute for Environmental Studies, 16-2, Onogawa, Tsukuba 305-0053, Ibaraki, Japan.

R.E. Shetter, Atmospheric Chemistry Division, National Center for Atmospheric Research, 1850 Table Mesa Drive, Boulder CO 80303.

H.B. Singh, NASA Ames Research Center, Moffett Field, CA 94035.

L. Jeagle, Department of Earth and Planetary Sciences, Harvard University, 29 Oxford Street, Pierce Hall, Cambridge, MA 02138.

A.M. Thompson, NASA Goddard Space Flight Center, Code 916, Greenbelt, MD 20771-0001.

M.J. Mahoney, Jet Propulsion Laboratory, 4800 Oak Grove Drive, Pasadena, CA 91109-8099.

S.C. Liu, School of earth and Atmospheric Sciences, Georgia Institute of Technology, 212 Bobby Dodd Way, Atlanta, GA 30332-340.

## Figure captions

Figure 1a. Profiles of $NO_x$ mixing ratios for air masses where 100 ppbv < $O_3$ < 200 ppbv and 200 ppbv < $O_3$. The median values at each 1 km step are also shown. The bars indicate central 67 % values.

Figure 1b. Same as Figure 1a but for $\Delta NO_y$ values. The values above 8.5 km are shown.

Figure 2. $NO_x$ mixing ratios plotted versus $\Delta NO_y$ above 9.5 km. The $\Delta NO_y$ values are the calculated increases in $NO_y$ along five-day back trajectories. Where 100 ppbv < $O_3$ < 200 ppbv, the data points are classified according to the time (T) required to increase the $\Delta NO_y$ values by 50 %. 0 < T < 1 day (closed circles), 1 <T< 2 days (open circles), and 3 < T <.5 days (crosses).

Figure 3. $NO_x$ mixing ratio plotted versus CN mixing ratios observed above 9.5 km (closed circles). The least square fitted line is shown as a solid line. The median $NO_x$–CN relationship obtained from aircraft exhaust plumes is shown as a dashed line.

Figure 4. $NO_x$ mixing ratios plotted versus the nonvolatile/total CN ratios. The points where $\Delta NO_y$ > 100 pptv and $\Delta NO_y$ < 100 pptv are shown as closed circles and open circles, respectively. The median values obtained from aircraft exhaust plumes are shown as large closed circles.

Table 1. Background (BG), median (MED), and average values of CN, $NO_x$, and $NO_x/NO_y$ ratio observed above 9.5 km where $100 < O_3 < 200$ ppbv. The uncertainties in the background values were defined as the 1-$\sigma$ standard deviation of the differences between the observed values and those calculated from equations (1)–(3) where $\Delta NO_y <$ 50 pptv.

| | CN ($cm^{-3}$) | $NO_x$ (pptv) | $NO_x/NO_y$ |
|---|---|---|---|
| BG | 833 ± 310 | 89 ± 37 | 0.13 ± 0.052 |
| MED | 1294 | 168 | 0.23 |
| Average ± 1$\sigma$ | 1380 ± 647 | 166 ± 83 | 0.22 ± 0.086 |
| MED–BG | 467 | 79 | 0.10 |
| (MED–BG)/BG | 56 % | 89 % | 77 % |

Fig. 19

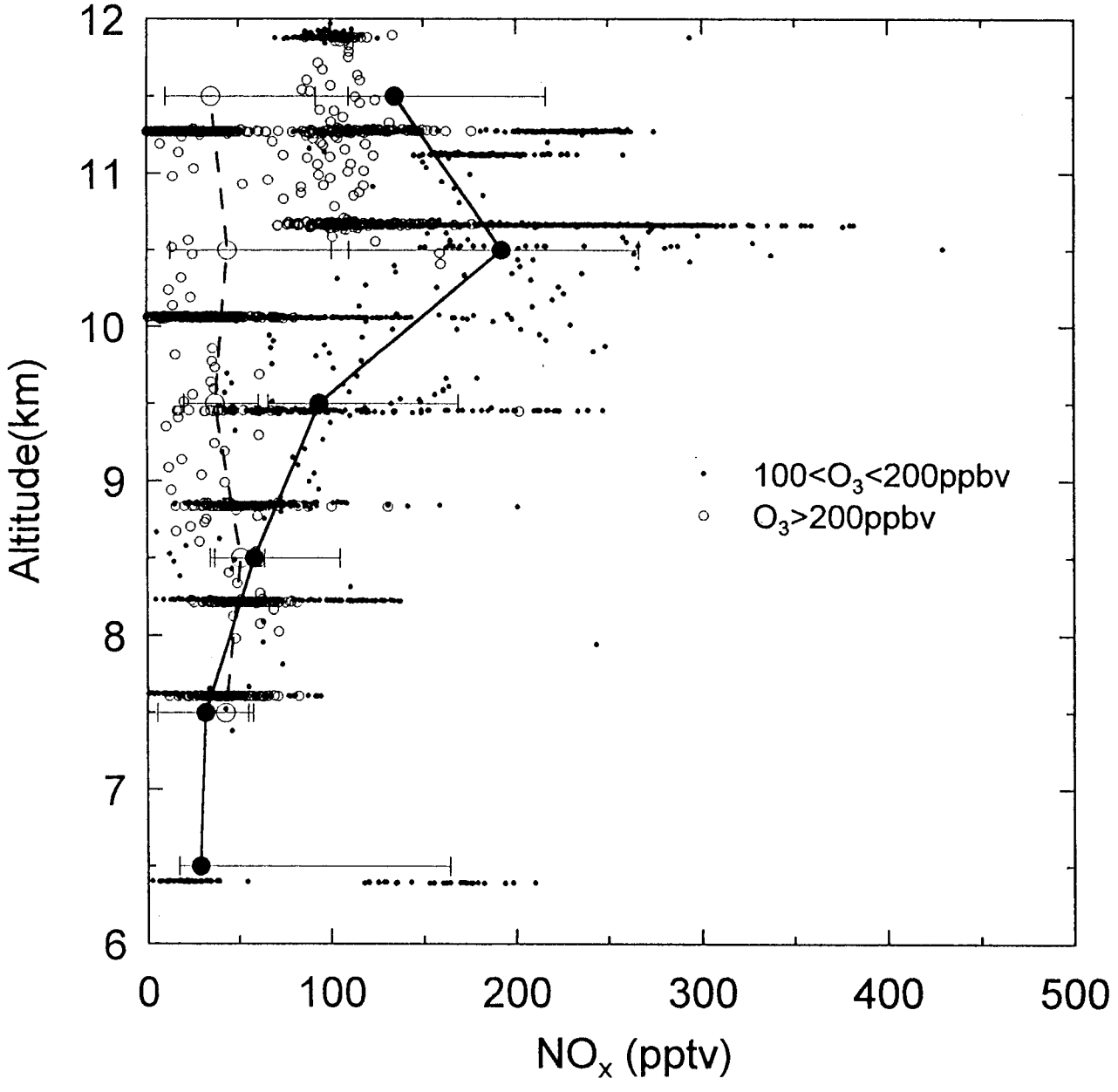


median and 67% value
No lightning, SZA<87deg
Without spike and intrusion
10 second average
Plot: 981223
Data: all_mg10_N1
Name: NOx-Alt(med_measCoz).QPC

Fig. 1b

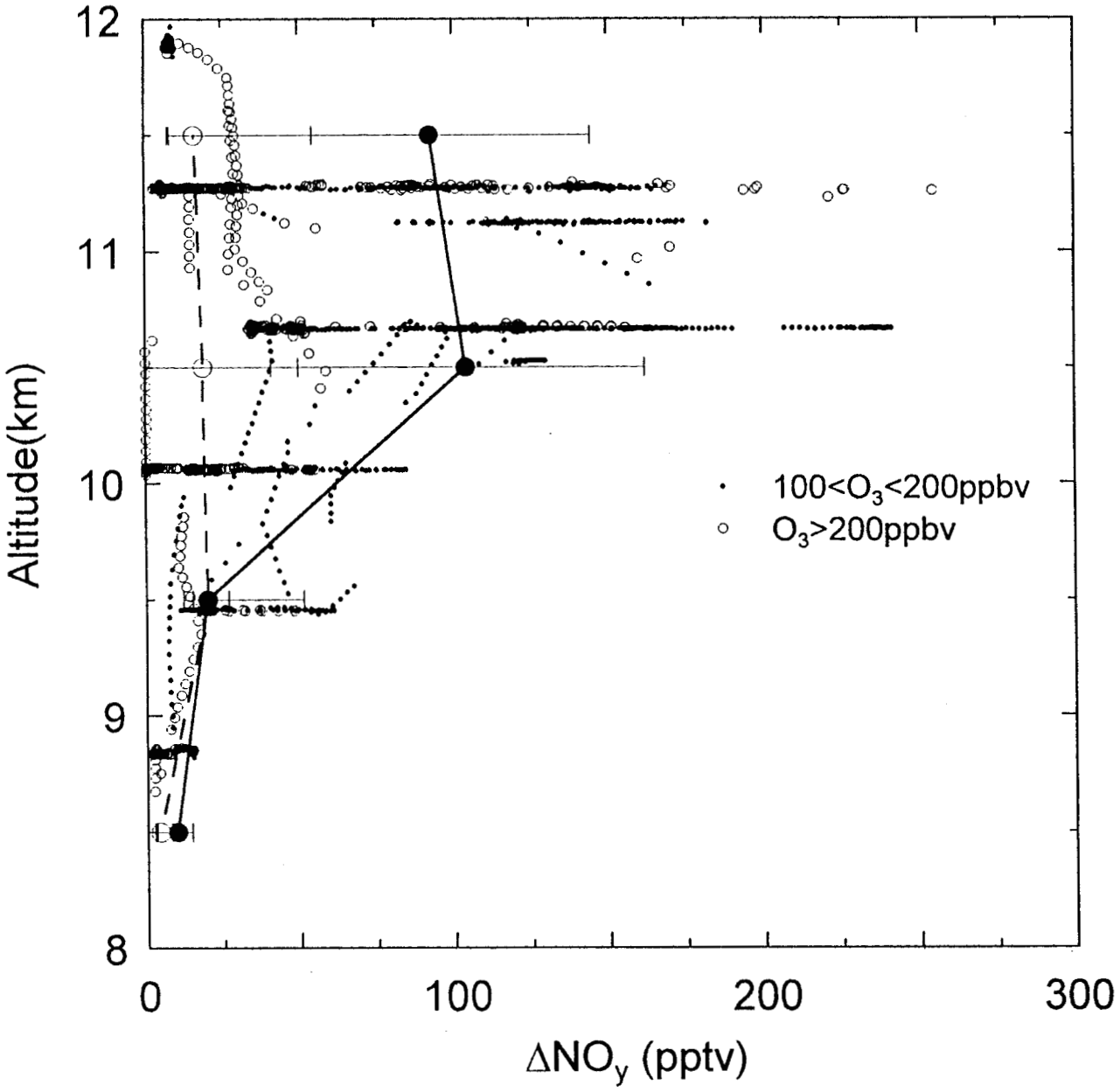


5day ΔNOy(No damping, kinematic)
median and 67% value
No lightning, SZA<87deg
Without spike and intrusion
10 second average
Plot: 981224,
Data: all_mg10_N1
Name: d5NOy-Alt(med_measCoz).QPC

F17.2

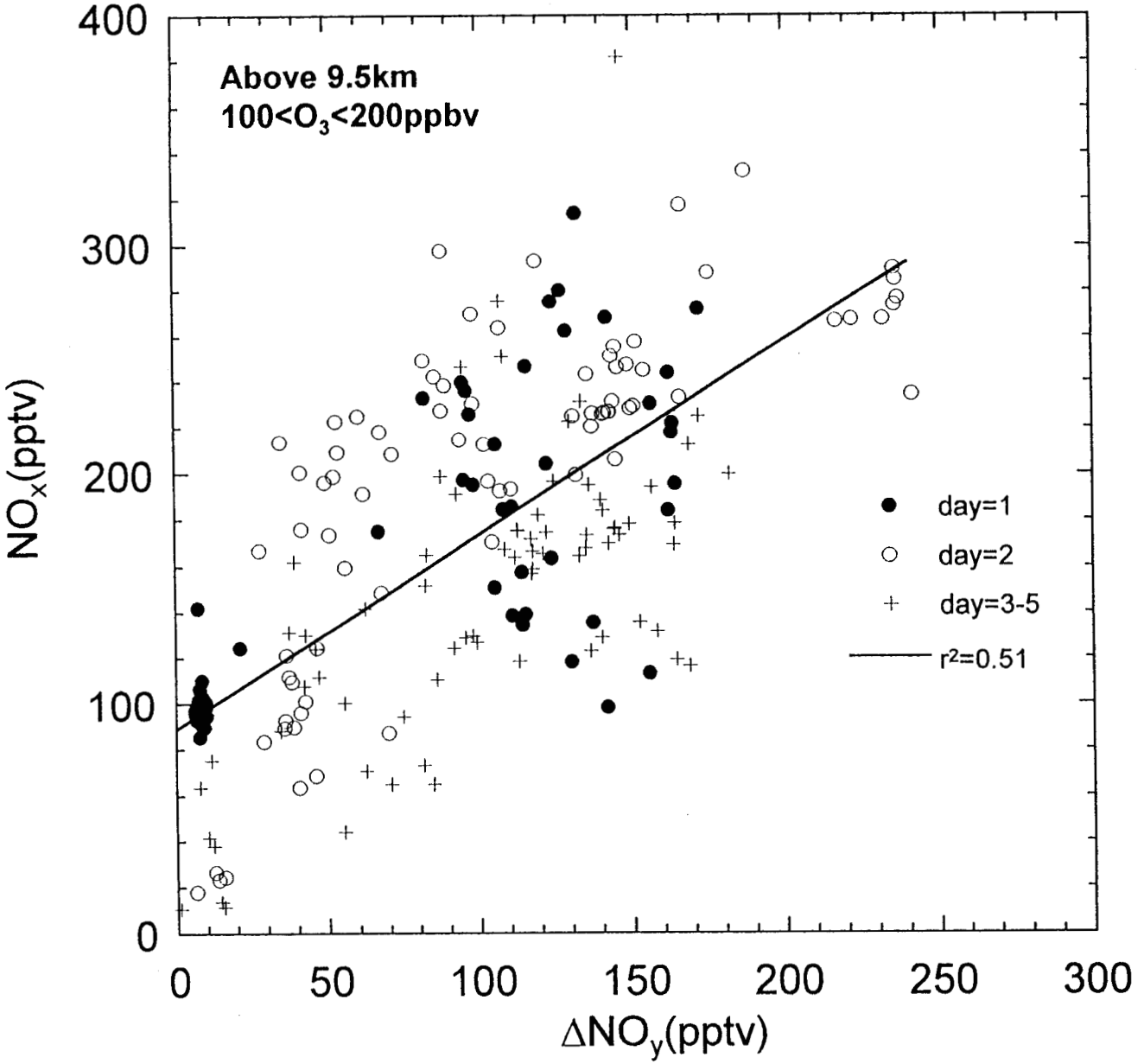


No lightning, without spikes and intrusion
5 days ΔNOy (No damping, kinematic)
1 minute average
Plot: 981223
Data: amg10_1MZm9.5
Name: d5NOy-NOx(Cday).QPC

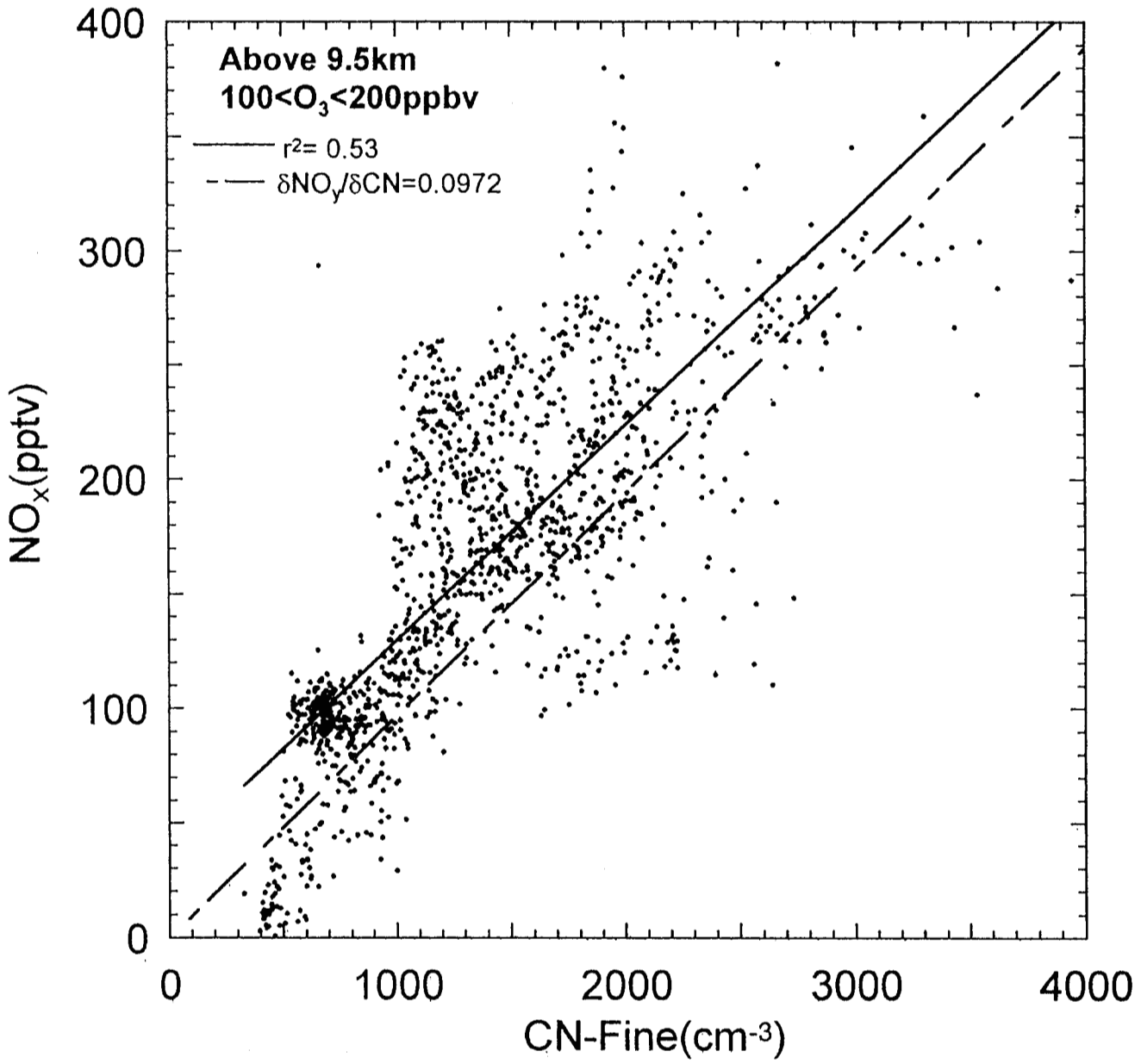


No lightning, SZA<87deg
without spike and intrusion
10 second average
Plot: 981223
Data: amg10_N1Zm9.5
Name: Fine-NOx.QPC

Fig. 4

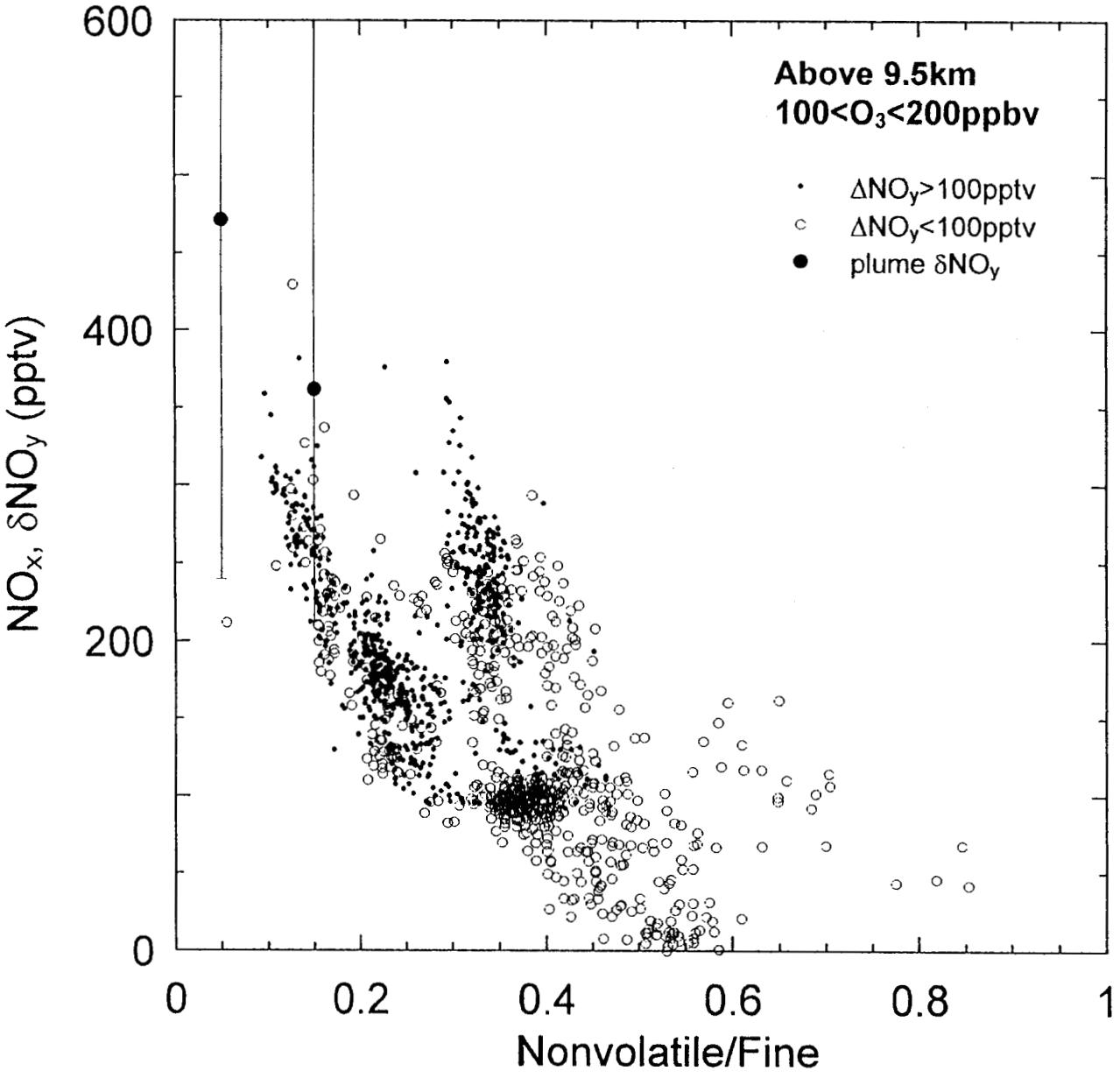


No lightning,SZA<87deg
without spike and intrusion
5 days ΔNOy (No damping, kinematic)

10 second average
Plot: 981224
Data: amg10_N1Zm9.5
Name: NV_F-NOx(CdNOy).QPC